Redox Biology 69 (2024) 103016

Contents lists available at ScienceDirect

Redox Biology

journal homepage: www.elsevier.com/locate/redox

M2 macrophage exosome-derived lncRNA AK083884 protects mice from CVB3-induced viral myocarditis through regulating PKM2/HIF-1α axis mediated metabolic reprogramming of macrophages

Yingying Zhang [a,b,d,e,1], Liangyu Zhu [a,b,c,1], Xueqin Li [a,b,c,d,f,1], Chang Ge [g,1], Weiya Pei [a,b,c,d], Mengying Zhang [a,b,c,d], Min Zhong [a,b,c,d], Xiaolong Zhu [a,b,c,d,f,**], Kun Lv [a,b,c,d,e,f,*]

[a] Anhui Province Key Laboratory of Non-coding RNA Basic and Clinical Transformation, Wuhu, PR China
[b] Key Laboratory of Non-coding RNA Transformation Research of Anhui Higher Education Institutes (Wannan Medical College), Wuhu, PR China
[c] Central Laboratory, The First Affiliated Hospital of Wannan Medical College (Yijishan Hospital of Wannan Medical College), Wuhu, PR China
[d] Non-coding RNA Research Center of Wannan Medical College, Wuhu, PR China
[e] Department of Laboratory Medicine, The First Affiliated Hospital of Wannan Medical College (Yijishan Hospital of Wannan Medical College), Wuhu, PR China
[f] Anhui Province Clinical Research Center for Critical Respiratory Medicine, Wuhu, PR China
[g] Department of Psychology, Zhejiang Sci-Tech University, Hangzhou, PR China

ARTICLE INFO

Keywords:
Exosomes
Long non-coding RNA
AK083884
Metabolic reprogramming
Viral myocarditis

ABSTRACT

Viral myocarditis (VM) is a clinically common inflammatory disease. Accumulating literature has indicated that M2 macrophages protect mice from Coxsackievirus B3 (CVB3)-induced VM. However, mechanisms that underlie M2 macrophages alleviating myocardial inflammation remain largely undefined. We found that M2 macrophage-derived exosomes (M2-Exo) can effectively attenuate VM. The long non-coding RNA (lncRNA) AK083884 in M2-Exo was found to be involved in the regulation of macrophage polarization by exosome lncRNA sequencing combined with in vitro functional assays. M2-Exo-derived AK083884 promotes macrophage M2 polarization and protects mice from CVB3-induced VM. Furthermore, we identified pyruvate kinase M2 (PKM2) as a protein target binding to AK083884 and found that PKM2 knockdown could promote macrophages to polarize to M2 phenotype. Intriguingly, functional assay revealed that downregulation of AK083884 promotes metabolic reprogramming in macrophages. In addition, co-immunoprecipitation was performed to reveal AK083884 could interact with PKM2 and inhibition of AK083884 can facilitate the binding of PKM2 and HIF-1α. Collectively, our findings uncovered an important role of M2-Exo-derived AK083884 in the regulation of macrophage polarization through metabolic reprogramming, identified a new participant in the development of VM and provided a potential clinically important therapeutic target.

1. Introduction

Viral myocarditis (VM) is an inflammatory disease of the heart, which usually manifested as acute myocarditis and may further develop into chronic VM, dilated cardiomyopathy, and even heart failure. Coxsackievirus B3 (CVB3) is considered a critical pathogen of VM [1–3]. However, due to poor understanding of the pathogenic mechanism of CVB3-induced VM, there is currently no effective and specific treatments. Extensive clinical and experimental researches have shown that in addition to virus mediated direct damage, immune pathological cardiac inflammation is a critical pathogenic mechanism of CVB3-induced VM [4]. Therefore, immune regulation has become one of the most promising therapeutic strategies for combating VM [5–7]. Clarifying the mechanism of over-reactive cardiac immune response will contribute to better understand the critical pathogenic processes of VM and provide some clues for the development of new treatment strategies.

Macrophages have been shown to play a critical role in the development of VM. They are not only the first batch of inflammatory cells recruited to heart tissue, but also the main subpopulation of infiltrating cells in the early stage of VM [8–11]. Macrophages can be stimulated to

* Corresponding author. Anhui Province Key Laboratory of Non-coding RNA Basic and Clinical Transformation, Wuhu, PR China.
** Corresponding author. Anhui Province Key Laboratory of Non-coding RNA Basic and Clinical Transformation, Wuhu, PR China.
E-mail addresses: Zhuxlon3@126.com (X. Zhu), lvkun315@126.com (K. Lv).
[1] These authors contributed equally to this work.

https://doi.org/10.1016/j.redox.2023.103016
Received 16 November 2023; Received in revised form 15 December 2023; Accepted 25 December 2023
Available online 28 December 2023

classically activated M1 or alternatively activated M2 phenotypes based on the cardiac environment [12]. Lipopolysaccharides (LPS) and interferons-γ (IFN-γ) induced M1 macrophages typically promote myocarditis and tissue damage by producing pro-inflammatory cytokines. Subsets of M2 macrophages include M2a, M2b, M2c, and M2d, with different properties such as cell markers, cytokines, and functions. M2a macrophages can promotes cell growth, tissue repair, and endocytosis. M2b macrophages play a role in regulating immune response and inflammation. The characteristic of M2c macrophages is the high expression anti-inflammatory IL-10, TGF-β, CCL16, CCL18, and Mer receptor tyrosine kinase (MerTK), among which MerTK can promote phagocytosis of apoptotic cells. M2d macrophages activated by TLR antagonists, IL-6, and adenosine. Adenosine promotes the expression of IL-10 and VEGF, which can exacerbate angiogenesis and tumor progression. In our study, we used IL-4 as stimuli to induce macrophage toward M2a polarization, with the high expression of Arg1, YM1, FIZZ1, and CD206 [13–15]. Our previous studies, as well as other studies, have demonstrated that M1 macrophages significantly exacerbate VM, while M2 macrophages attenuate myocarditis [9,16–21]. The transition in the balance between M1 and M2 macrophages conduce to an increase in M2 macrophage infiltration, which may be a potential target for VM therapy.

Exosomes are cell-derived nanovesicles, approximately 30–150 nm in size, that exist in all tissue, body fluids (including blood and urine), and cell culture medium. Many reports have shown that exosomes, as functional paracrine units of cells, can partially replicate the bioactive functions of their parent cells, indicating that they may provide a substitute, cell-free therapeutic option [22–25]. The mechanism of exosome mediated physiological and pathological processes mainly depend on the transfer of exosome cargos, including non-coding RNA (ncRNA) and proteins, to recipient cells. Therefore, the composition and biological activity of exosomes are largely decided by the physiological status of their parent cells [26–29].

Recent studies have unveiled that the biological molecular composition of exosomes released by macrophages reflects the special characteristics of original cells: powerful immune or inflammatory regulatory activity [30]. The function of exosomes or extracellular vesicles originated from M1 or M2 phenotype macrophages has recently been clarified [31–37]. For example, exosomes derived from M1 macrophages in obese adipose tissue that contain abundant miRNAs, such as miR-155 and miR-146a, lead to insulin resistance in mice [32]. Liu et al. showed that M1 macrophage-released exosomes inhibit angiogenesis and aggravate cardiac dysfunction in a myocardial infarction microenvironment [35]. In addition, Wang et al. found that miRNA-421-3p-enrichment small extracellular vesicles released from M2 bone marrow-derived macrophages (BMDMs) alleviate apoptosis and facilitate the recovery of motor function via suppression of mTOR in spinal cord damage [36]. Bouchareychas et al. reported that exosomes of M2 macrophage decrease hematopoiesis and the inflammatory status of circulating monocytes and macrophages in atherosclerotic plaques [37]. However, the precise function of M2 macrophage-derived exosomes (M2-Exo) and the impact of their lncRNA cargo in VM have not been reported.

In this study, we hypothesized that M2-Exo may have better therapeutic activity by controlling the inflammatory properties of cardiac macrophages of VM. Our findings also showed that M2-Exo promote inflammation resolution by regulating macrophage toward an M2 phenotype in VM mice via the delivery of lncRNA cargo. The favorable properties exerted by M2-Exo, along with their ease of generation of lncRNA cargo, provide a new therapeutic strategy for the therapy of inflammation, including in the cardiovascular system.

2. Materials and methods

2.1. Mice

BALB/c male mice (6–8 weeks of age, 18–20 g in weight) were acquired from Experimental Animal Center of Qinglongshan (Nanjing, China) and raised in a specific-pathogen-free (SPF) mouse colony. All of the animal experimental procedures were guided by the Care and Use of Laboratory Animals (Ministry of Health, China, 1998). The protocols of all of the animal experiments were obtained permission from the Animal Ethics Committee of the Yijishan Hospital of Wannan Medical College.

2.2. Primary BMDMs

Primary BMDMs isolation was described previously [16,17]. BMDMs were separated from the mice femurs and tibias under sterile conditions. BMDMs were seeded in 6-well plates and cultured in Dulbecco's Modified Eagle's medium (DMEM, Gibco, Life Technologies, NY, USA) containing 20 % fetal bovine serum (FBS, Gibco) and 20 % L929 cell supernatant at 37 °C and in a 5 % CO2 incubator (M0). Seven days later, the cells were transferred in fresh RPMI-1640 medium containing 10 % FBS for 24 h. BMDMs were cultured with DMEM medium (10 % FBS) supplemented with 100 ng/ml LPS (Sigma, USA) plus 20 ng/ml IFN-γ (PeproTech, Cranbury, NJ, USA) for 24 h to activate M1 polarization or 20 ng/ml IL-4 (PeproTech) for 48 h to activate M2 polarization.

2.3. Separation of M2-Exo

For exosome identification, the exosomes were separated by Exosome Isolation Kit (UR52121; Umibio; Shanghai, China) following with the manufacturer's instructions. Briefly, the DMEMs medium was replaced with exosome-depleted FBS (Gibco) when M2 macrophages reached 80 % confluence, and then 48 h later, the supernatant was collected. Subsequently, the supernatant was centrifuged at 3000×*g*, 4 °C for 10 min and then at 10,000×*g*, 4 °C for 20 min to eliminate cells and debris in the precipitate. The supernatant was incubated with Kit reagents in proportion at 4 °C for up to 2 h and centrifuged at 10,000×*g*, 4 °C for 60 min. The exosome in the precipitate was washed once with 1 × PBS. After centrifugation at 3000×*g* for 10 min at 4 °C, the exosome pellet was dissolved in 100 μl PBS and stored at −80 °C before use. For M2-exo used in functional assays, differential ultracentrifugation was used for M2-Exo isolation. Briefly, the M2 macrophages culture supernatant was centrifuged at 3000×*g*, 4 °C for 10 min and then at 10,000×*g*, 4 °C for 20 min to eliminate cells and debris in the precipitate. After filtering through a 0.22-μm filter, the supernatant was ultracentrifuged at 110,000×*g* for 2 h at 4 °C (Optima XPN-100 Ultracentrifuge, Beckman Coulter, USA) to acquire M2-Exo.

2.4. Identification of M2-Exo

Nanoparticle tracking analysis (NTA) was used to determine the size distribution of the M2-Exo. ZetaView system was calibrated by 100-nm polystyrene particles. Then, the exosome pellet suspended in PBS was injected into the Particle Tracking Analyzer (Particle Metrix, Zetaview, Germany). The particle size of the M2-Exo was analyzed by the ZetaView system.

The size distribution of the M2-Exo was measured using flow cytometry. Briefly, 100 nm and 200 nm polystyrene beads (part number: 6,602,336, Beckman Coulter) were used, and M2-Exo were detected with the proper order by flow cytometry (CytoFLEX, Beckman Coulter). The data was analyzed using CytExpert (Beckman) and Kaluza 2.1 software (Beckman Coulter). The M2-Exo size and morphology were observed by transmission electron microscopy (HITACHI, Tokyo, Japan). The marker proteins of exosomes were detected by Western blot. Bicinchoninic Acid (BCA) Protein Assay kit (Beyotime, Shanghai, China) was used to measure the protein concentration of the isolated M2-Exo

fraction following the manufacturer's instructions. M2-Exos (10 μg protein) were lysed in laemmli buffer (Sigma, USA), separated by SDS-PAGE, and transferred onto a 0.22-μm nitrocellulose (NC) filter membrane (Millipore, Bedford, MA, USA). The NC filter membranes were incubated with primary antibodies: Alix (Abcam, MA, USA), Annexin V (Abcam), CD54/ICAM-1 (Abcam), CD9 (Abcam), TSG101 (Abcam), EpCAM (Abcam), HSP70 (Abcam), and Flotillin-1 (Abcam).

2.5. Viral myocarditis (VM) model

To induce the VM model, mice were intraperitoneally injected with CVB3 (Nancy strain, a gift of Professor Wei Hou, School of Basic Medical Sciences, Wuhan University). Before infection, the virus titer was routinely measured by a 50 % tissue culture infectious dose (TCID50) assay of HeLa cells (ATCC number: CCL-2) monolayers following with previously procedures. Then 1×10^5 plaque-forming units (PFU) of CVB3 were diluted in 100 μl of PBS and injected intraperitoneally as described in a previous study [16]. Seven days later, a successful VM model was confirmed by histopathological examination via hematoxylin and eosin (H&E, YEASEN, China) staining.

2.6. Uptake of M2-Exo

To verify the cardioprotection of M2-Exo *in vivo*, mice were intramyocardially injected with M2-Exo or PBS on day 0 of VM model construction. The intramyocardial injection of M2-Exo was conducted by using minimally invasive image guided injection system under transthoracic echocardiography with Vevo 3100 LT with an MX550D linear array transducer (FUJIFILM VisualSonics). Briefly, mice were anesthetized with 2 % isoflurane, following inhalation of 1–2% isoflurane, the transthoracic B-mode echocardiography was performed. Then, M2-Exo dissolved in 50 μl PBS (1.2×10^7 particles/μl) was administered evenly intramuscularly by 30 G needle into five locations along the anterior wall of the left ventricles's border zone with the help of minimally invasive image guided injection system.

For uptake of M2-Exo *in vitro*, PKH26-red (Umibio, Shanghai, China)-labeled M2-Exo were added with BMDMs at a dose of 6.0×10^8 particles/mL. Following incubation at 37 °C for 24 h, BMDMs were washed three times with PBS to remove excess M2-Exo and fixed with 4 % paraformaldehyde for 10 min. After staining with DAPI for 5 min, BMDMs images were acquired with an LSM800 confocal microscope (Zeiss, Mainz, Germany).

2.7. Macrophage clearance assays

For macrophage clearance assays, 200 μl of clodronate liposomes (5 mg/ml) was injected into the tail vein on alternate days. The injection schedule was established according to the experimental requirements, and macrophage clearance efficiency was measured by flow cytometry.

2.8. Evaluation of cardiac dysfunction

We performed H&E staining to evaluate the histopathology of the VM model. First, mice hearts were collected and fixed with 10 % formalin. After paraffin embedding, the tissues were cut in sections of 5-μm thick and stained with H&E (YEASEN). Inflammatory cell infiltration in transverse tissue sections of the heart was determined by two pathologists in a blinded fashion.

The cTnI level in serum was measured with a DXI800 (Beckman Coulter) immunology analyzer from Yijishan Hospital. The concentrations of IFN-γ, IL-4, and IL-13 in cell supernatant were detected by cytokine ELISA kits (R&D Systems) following with the manufacturer's instructions.

Transthoracic echocardiography was performed using Vevo 3100 LT with an MX550D linear array transducer (FUJIFILM VisualSonics). Cardiac function was measured on left ventricular long axis B-mode images.

2.9. Western blot (WB)

Cells or exosomes were collected and lysed in Laemmli buffer (Sigma, USA). The protein concentration was determined with BCA Protein Assay kit (Beyotime). Protein lysates were separated by SDS-PAGE and transferred onto NC filter membrane (Millipore). Then the NC filter membrane was subsequently incubated with the primary antibody: iNOS (Abcam), Arg1 (Abcam), p-STAT1 (Abcam), p-STAT6 (Abcam), STAT1 (Abcam), STAT6 (Abcam), SOCS2 (Abcam), PKM2 (Cell Signaling Technology, CST, Danvers, MA, USA), HIF-1α (Invitrogen, Life Technologies, Carlsbad, CA, USA), β-actin (Abcam). β-actin was used as a control. After incubation with secondary antibodies and ECL (enhanced chemiluminescence, Millipore), the protein bands were captured by Bio-Rad ChemiDoc Touch Imaging System (Bio-Rad, Hercules, CA, USA). Quantitative analysis of protein bands was conducted with ImageJ software.

2.10. Flow cytometry analysis

Macrophage phenotypes were determined by flow cytometry. The single-cell suspensions of the heart were conducted by gentleMACS™ tissue dissociators and tubes (Miltenyi Biotec, Auburn CA) and stained with anti-CD11b (eBioscience; BD Pharmingen; Biolegend) for 30 min. Following with fixation and permeabilization, cells were stained with anti-iNOS (eBioscience) and anti-Arg1 or anti-CD206 (Thermo Flyscience). After staining, the samples were measured by CytoFLEX flow cytometry (Beckman Coulter). The data were analyzed with CytExpert software (Beckman Coulter).

2.11. Fluorescence in situ hybridization (FISH) and immunofluorescence

FISH and protein immunofluorescence analysis were performed as previously described [16]. For FISH, hybridization was carried out at 60 °C with fixed culture cells. For immunofluorescence, fixed cells were incubated with the primary antibody at 37 °C. Then 2 h later, cells were treated with the secondary antibody for 1 h at 37 °C. Cellular DNA was finally stained with DAPI (Sigma). The antibody details for these assays were used as follows: iNOS antibody (Abcam), arginase antibody (Abcam), CD68 antibody (Abcam). The FISH probe which targeting AK083884 was purchased from RiboBio (Guangzhou, China). Images were captured and analyzed with a Zeiss LSM800 confocal microscope.

2.12. M2-Exo lncRNA sequencing

The sequencing of lncRNA in M2-Exo was performed by RiboBio Co. A total of 10 ml culture media contained 10 % exosome-depleted FBS (Gibco) of M2 macrophages was mixed with RiboTM Exosome Isolation Reagent, and exosome isolation was performed according to the manufacturer's instructions (RiboBio, Guangzhou, China). Exosomal RNA was extracted with Trizol Reagent (Invitrogen) and used for library preparation and sequencing. Library preparation and sequencing were performed at RiboBio. Briefly, RNA was fragmented to approximately 200 bp. Subsequently, the collected RNAs were subjected to first strand and second strand cDNA synthesis followed by adaptor ligation and enrichment with a low-cycle according to the instructions provided with the NEBNext® Ultra™ RNA Library Prep Kit for Illumina (NEB, USA). The purified library products were evaluated using the Agilent 2200 TapeStation and Qubit®2.0 (Life Technologies, USA) and then sequencing (2×150 bp) using a HiSeq30000. The clean reads were obtained after removal of reads containing adapter, ploy-N and at low quality from raw data. HISAT2 was used to align the clean reads to the mouse reference genome mm10 with default parameters. HTSeq was subsequently employed to convert aligned short reads into read counts for each gene model. Differential expression was assessed by DEseq

using read counts as input. The Benjamini-Hochberg multiple test correction method was enabled. Differentially expressed genes were chosen according to the criteria of fold change >2 and adjusted p-value <0.05. The raw data have been uploaded in the Genome Sequence Archive of the China National Center for Bioinformation (GSA: 314 CRA009657).

2.13. Transfection of siRNAs and lncRNA smart silencer

PKM2 siRNA and lncRNA AK083884 smart silencer were synthesized by RiboBio Co. BMDMs were transfected with siRNA or lncRNA smart silencer using riboFECTTM CP Transfection Kit (RiBoBio) following with the manufacturer's instructions. 48 h later, the cells were used for the subsequent experiment.

2.14. Lentiviral infection

For overexpression of SOCS2, the pSLenti-CMV-SOCS2 lentivirus expression vector were ordered from OBIO company. For lentiviral infection, BMDMs were infected with pSLenti-CMV-SOCS2 lentivirus expression vector (MOI = 100) following with the manufacturer's instructions. 48 h later, the cells were used for the subsequent experiment.

2.15. Real-time quantitative PCR (qRT-PCR)

Total RNA from cells or tissues was extracted with Trizol reagent (Ambion, Life Technologies, CA, USA) following with the manufacturer's instructions. Then the total RNA was synthetized to cDNA by using the QuantiTect Reverse Transcription Kit (Thermo Scientific, Lithuania, USA). SYBR Green PCR Master Mix (Qiagen, Hilden, Germany) was used to perform qRT-PCR on Bio-Rad CFX96 RT-PCR System. GAPDH was used for normalization. The mRNA or lncRNA expression levels were analyzed with the comparative cycle threshold ($2^{-\Delta\Delta CT}$) method. Primers used are detailed in Supplementary Table 1.

2.16. Arginase activity assay

BMDMs were treated with M2-Exo (si-NC) or M2-Exo (si-AK083884) for 48 h, followed by activation with IL-4 for an additional 24 h. Then the arginase activity was detected. Briefly, BMDMs were lysed by 0.1 % Triton X-100 for 30 min and then mixed with an equal volume of 50 mM Tris–HCl plus 10 mM $Cl_2Mn{\cdot}4H_2O$ (pH 7.5) at 55 °C for 10 min. L-arginine hydrolysis was conducted by 0.5 M l-arginine (pH 9.7) and stopped with [$H_2SO_4/H_3PO_4/H_2O$ (1:3:7, v/v/v)] solution and 9 % 2-isonitrosopropiophenone. The samples were measured by a microplate reader (BioTek Epoch, Winooski, Vermont) at 540 nm. With the generation of a standard curve, the final concentrations of urea were calculated.

2.17. Seahorse extracellular flux analysis

The extracellular acidification rate (ECAR) and oxygen consumption rate (OCR) of M2 macrophages were determined using a Seahorse XFe24 extracellular flux analyzer (Agilent Technologies, CA, USA). BMDMs, which were transfected with lncRNA smart silencer and treated with IL-4, were seeded in an XF 24-well plate (1×10^4 cells per well) referring to the standard instructions. The Seahorse XF Cell Mito Stress Test kit (Agilent) and XF Glycolysis Stress Test kit (Agilent) were used for the measurement of OCR and ECAR, respectively. A quantity calculation from the result was achieved by Seahorse WAVE software (Agilent) normalized to cell number and calculated as mpH/min or pmoles/min.

2.18. RNA pull-down

Pull-down assay was conducted using biotinylated RNA. Briefly, biotin-labeled RNA was transcribed with a Transcript Aid T7 High Yield Transcription Kit (Thermo Fisher) *in vitro*. After treatment with RNase-free DNase I, biotin-labeled RNA was purified using an RNeasy Mini Kit (Qiagen). Then, the biotin-labeled AK083884 sense and antisense RNA were synthesized by the Biotin RNA Labeling Mix kit (Roche, Mannheim, Germany) and SP6 RNA polymerase (Roche). Streptavidin magnetic beads (Invitrogen) were used to catch the biotin-labeled AK083884 probe. Then, the biotinylated RNA compound was incubated with purified proteins from M2 macrophages. The pull-down complexes were detected by WB. Mass spectrometry (MS) technique was used to identify AK083884-interacting proteins based on peptide polypeptide alignments results.

2.19. RNA-binding protein immunoprecipitation (RIP)

RIP was primarily used to verify the interaction between protein PKM2 and AK083884. The RNA obtained by immunoprecipitation was detected by qRT-PCR, and the product was guaranteed to be free of RNase following the Magna RIP™ RNA-Binding Protein Immunoprecipitation kit (Millipore).

2.20. Co-immunoprecipitation (co-IP)

Immunoprecipitation was conducted using the Pierce co-IP kit (Thermo Scientific). Briefly, M2 macrophages were lysed following the manufacturer's protocol, and aliquot (30 μL) of lysate input was saved for extraction of input protein. Precipitation of PKM2 immune complexes was performed by anti-PKM2 antibody coupled with protein A/G Plus agarose beads for 2 h at 4 °C, and a control IgG antibody was used for the control samples. Finally, the immunoprecipitated samples were analyzed for PKM2 and HIF-1α protein expression by WB.

2.21. Statistical analyses

Data are displayed as the mean ± SD. Statistical analysis of the data was used a two-tailed independent Student's *t*-test or ANOVA analysis. The survival status of the mice was tested by Kaplan–Meier (K–M) plots, and survival durations were analyzed using the log-rank test. All of the analyses were employed with GraphPad Prism v5.0 (GraphPad Software). $P < 0.05$ was assumed statistically significant.

3. Results

3.1. M2-Exo was characterized by NTA, flow cytometry, TEM, and WB

Exosomes were isolated from the medium supernatants of M2 macrophages using exosome precipitation solution kit. Then the morphology and phenotypes of isolated exosomes were characterized. We conducted NTA and flow cytometry to measure the size distribution of the exosomes. The diameters of almost all of the exosomes ranged from 30 to 150 nm (Figs. S1A and 1B). TEM showed that the exosomes were cup-shaped, membrane-bound, and had a diameter of approximately 100 nm (Fig. S1C). Furthermore, Western blot analysis indicated that the particles were highly enriched with Alix, Annexin V, CD54/ICAM-1, CD9, TSG101, EpCAM, HSP70, and Flotillin-1, which were exosome marker proteins (Fig. S1D). Therefore, the above property analysis indicated that M2-Exo collected in our study were exosomes.

3.2. M2-Exo attenuated myocardial inflammation and cardiac dysfunction in VM mice

To investigate the role of M2-Exo in VM, exosomes were delivered to the myocardium. The dose of exosomes was based on our preliminary dose-ranging experiment. Mice were administered M2-Exo (6.0×10^8 particles) or PBS via an intramyocardial injection on the first day of VM model. Results showed that M2-Exo alleviated myocardial inflammation, such as the restricted foci of inflammation and reduced

inflammation area (Fig. 1A). In accordance with this result, M2-Exo significantly reduced the serum cTnI levels and body weight loss related to systemic illness (Fig. 1B and C). Furthermore, M2-Exo significantly improved the survival rate of VM model from approximately 50 %–75 % (Fig. 1D). We also measured the concentrations of pro-inflammatory cytokine (IFN-γ) and anti-inflammatory cytokine (IL-4 and IL-13) in the heart tissues of VM mice following M2-Exo or PBS treatment. The results showed that M2-Exo injection decreased IFN-γ production and increased the levels of IL-4 and IL-13 (Fig. 1E). Fractional shortening and ejection fraction have a role in predicting outlook in cardiac function. M2-Exo improved cardiac function by increasing fractional shortening (%) and ejection fraction (%) in VM mice surviving for 5 weeks (Fig. 1F). Collectively, these results suggested that M2-Exo exerted protective effects by reducing mortality and cardiac dysfunction of CVB3-induced VM mice.

3.3. Clodronate liposomes reduced therapeutic effects of M2-Exo through depleting macrophages

Macrophages play a pivotal role in mediating VM. As such, we investigated the role macrophages play in M2-Exo therapy. Clodronate liposomes (clod lip) has become the agent of choice to selectively and specifically deplete macrophages [38]. We have confirmed that clod lip significantly reduced cardiac macrophage populations in the VM model using flow cytometry analysis (Fig. S2A). Then we examined whether clod lip weakens the cardioprotective effect of M2-Exo. As shown in the flow chart of Fig. S2B, M2-Exo- or PBS-treated VM model was constructed following clod lip injection at the assigned time point. Compared with PBS and clod lip treatment, myocardial inflammation in the VM model was not alleviated in the group treated with M2-Exo and clod lip (Fig. S2C). Altogether, these results indicated that macrophages were required for M2-Exo to exert cardioprotective effects.

3.4. M2-Exo promoted the transition of macrophages toward M2 phenotype during VM

More and more results have proved that macrophage polarization plays a critical role in the VM. We therefore examined whether M2-Exo could stimulate macrophages toward the M1 or M2 phenotype under VM. Flow cytometry analysis showed that the proportion of M1 macrophages ($CD11b^{+}iNOS^{+}$) was decreased in the hearts of M2-Exo-treated VM mice, while the proportion of M2 macrophages ($CD11b^{+}Arg1^{+}$) was increased (Fig. 2A). Furthermore, qRT-PCR analysis also showed M2-Exo treatment inhibited the expression of M1 marker (NOS2), while it induced the expression of M2 markers (Arg1, FIZZ1, and YM1) (Fig. 2B). Western blot analysis confirmed that the M1 marker iNOS had low expression and the M2 marker Arg1 had high expression in M2-Exo-treated VM mice (Fig. 2C). Fluorescence results showed that the co-localization of the M2 marker (Arg1) with the macrophage marker CD68 was significantly increased in heart tissue from M2-Exo-treated VM mice, but the co-localization of the M1 marker (iNOS) with CD68 was barely detected (Fig. 2D). These data indicated that M2-Exo treatment polarize macrophages away from the M1 phenotype and toward the M2 phenotype under VM.

3.5. LncRNA AK083884 was an effector candidate of M2-Exo-mediated macrophage polarization

Exosomes can mediate intercellular communication by exchanging lncRNAs between receptor cells. To explore the role of lncRNAs contributing to M2-Exo-induced cardioprotection, we performed a lncRNA profiling assay for M2-Exo by RiboBio. AK083884 is a special candidate as it is upregulated in M2 macrophages and enriched in M2-Exo (Fig. 3A). qRT-PCR further confirmed that AK083884 was highly expressed in M2 macrophages and M2-Exo (Fig. 3B and C). AK083884 is localized on chromosome 10 (chr10: 94870987–94874833) and is an approximately 3847 nt sequence derived from the intron 1 region of the encoded gene SOCS2 (Fig. 3D). SOCS2 is a key signaling molecule known to determine the polarization phenotype of macrophages [39]. An RNA FISH assay indicated that AK083884 was mainly located in the nucleus (Fig. 3E). Furthermore, the Coding Potential Calculator (CPC) software predicted that AK083884 has almost no protein encoding capability (Fig. 3F).

Subsequently, we further characterized the role of AK083884 in macrophage polarization. Compared with M1 macrophages, a time course assay showed that the expression of AK083884 was increased at 18 h and peaked at 30 h in M2 macrophages (Fig. 3G). We detected the AK083884 expression in macrophages following the dynamic process of macrophage re-polarization. We found that AK083884 expression in macrophages was increased during M1 polarization to M2 but decreased following M2 polarization to M1 (Fig. 3H and I). In addition, the expression of AK083884 was significantly decreased during VM (Fig. 3J). Together, our data demonstrated that AK083884 may play an important role in regulating macrophage polarization.

3.6. AK083884 was involved in the M2-Exo-mediated macrophage polarization in vitro

To further understand the functions of M2-Exo on the macrophage polarization, we constructed PKH26 (red)-labeled M2-Exo and evaluated the uptake effects of M2-Exo by macrophages *in vitro*. We found that M2-Exo were absorbed into macrophages and retained in the cytoplasm (Fig. 4A). To examine the role of AK083884 in M2-Exo, we inhibited AK083884 expression in M2-Exo by transfecting BMDMs with AK083884 smart silencer and subsequently purified the exosomes from the culture supernatants of M2 macrophages. The qRT-PCR showed that AK083884 expression was knocked down in M2-Exo (si-AK083884) (Fig. 4B). In addition, the expression of the M1 marker (NOS2) was increased, while M2 markers (Arg1, FIZZ1, and YM1) were decreased in BMDMs with M2-Exo (si-AK083884) treatment (Fig. 4C). Consistently, BMDMs with M2-Exo (si-AK083884) treatment showed upregulation of M1 markers (iNOS), as well as the downregulation of M2 marker (Arg1) and arginase activity (Fig. 4D and E). Taken together, these data indicated that the AK083884 in M2-Exo might be responsible for the regulation of macrophage polarization.

3.7. AK083884 in M2-Exo mediated STAT signaling through regulating SOCS2 expression

LncRNAs have been shown to regulate nearby genes in a positive or negative manner. AK083884 was derived from the intron 1 region of the encoded gene SOCS2. We investigated whether AK083884 influences SOCS2 expression. Similar to AK083884, the expression of SOCS2 also increased in M2 macrophages (Fig. 5A). qRT-PCR and WB showed that treatment of M2-Exo (si-AK083884) significantly inhibited the expression of SOCS2 in M2 macrophages (Fig. 5B and C).

Previous study suggested that there is a relationship between SOCS2 and STAT signaling pathways during macrophage polarization. SOCS-mediated signaling might inhibit the activation of the STAT signaling pathway, which is critical for the conversion of anti-inflammatory M2 macrophages [40]. Thus, we investigated the relationship between SOCS2 and STAT signaling pathways in macrophages. WB analysis revealed that the levels of phosph-STAT6 (p-STAT6) were significantly upregulated in BMDMs after M2-Exo treatment (Fig. 5D). Treatment of M2-Exo (si-AK083884) reduced the expression of p-STAT6 in M2 macrophages, while the expression levels of p-STAT6 were recovered after overexpression of SOCS2 (Fig. 5E). These results indicated that AK083884 shuttling by M2-Exo may regulate macrophage polarization via the SOCS2/STAT signaling pathway.

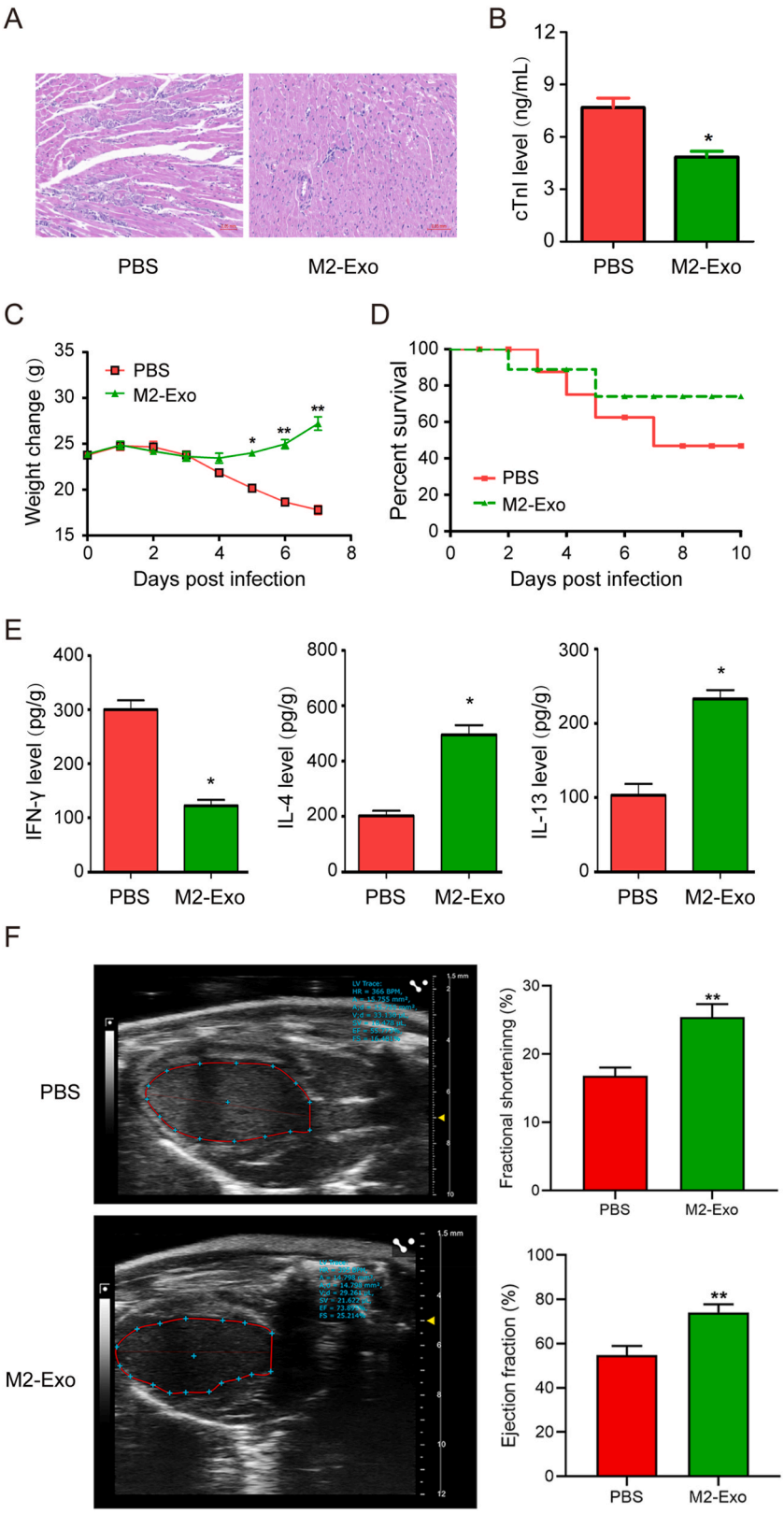

Fig. 1. Intramyocardial infusion of M2-Exo attenuates myocardial inflammation and cardiac dysfunction in VM mice. Mice were intramyocardially injected with PBS or M2-Exo when the VM model was constructed. The phenotypes of VM model were evaluated. (A) The heart was stained with H&E. Scale bar = 0.05 mm. (B) The serum level of cTnI was determined by ELISA. (C). The weight change in the mice. (D) The survival rate of the mice was determined at day 10 of VM model. The total number of mice for both PBS group and M2-Exo group were 20 mice, and the survival number of PBS group was 9 mice, while M2-Exo group was 16 mice on day 10 post infection. The Log-Rank P value was 0.044. (E) The levels of IFN-γ, IL-4, and IL-13 in the heart tissue of mice were detected by ELISA. (F) Echocardiographic examination was determined at week 5 (day 35). Fractional shortening and ejection fraction were determined by an ultrasound system. The experiment was repeated three times, with 8 mice in each group. Data are presented as the mean ± SD; *P < 0.05, **P < 0.01.

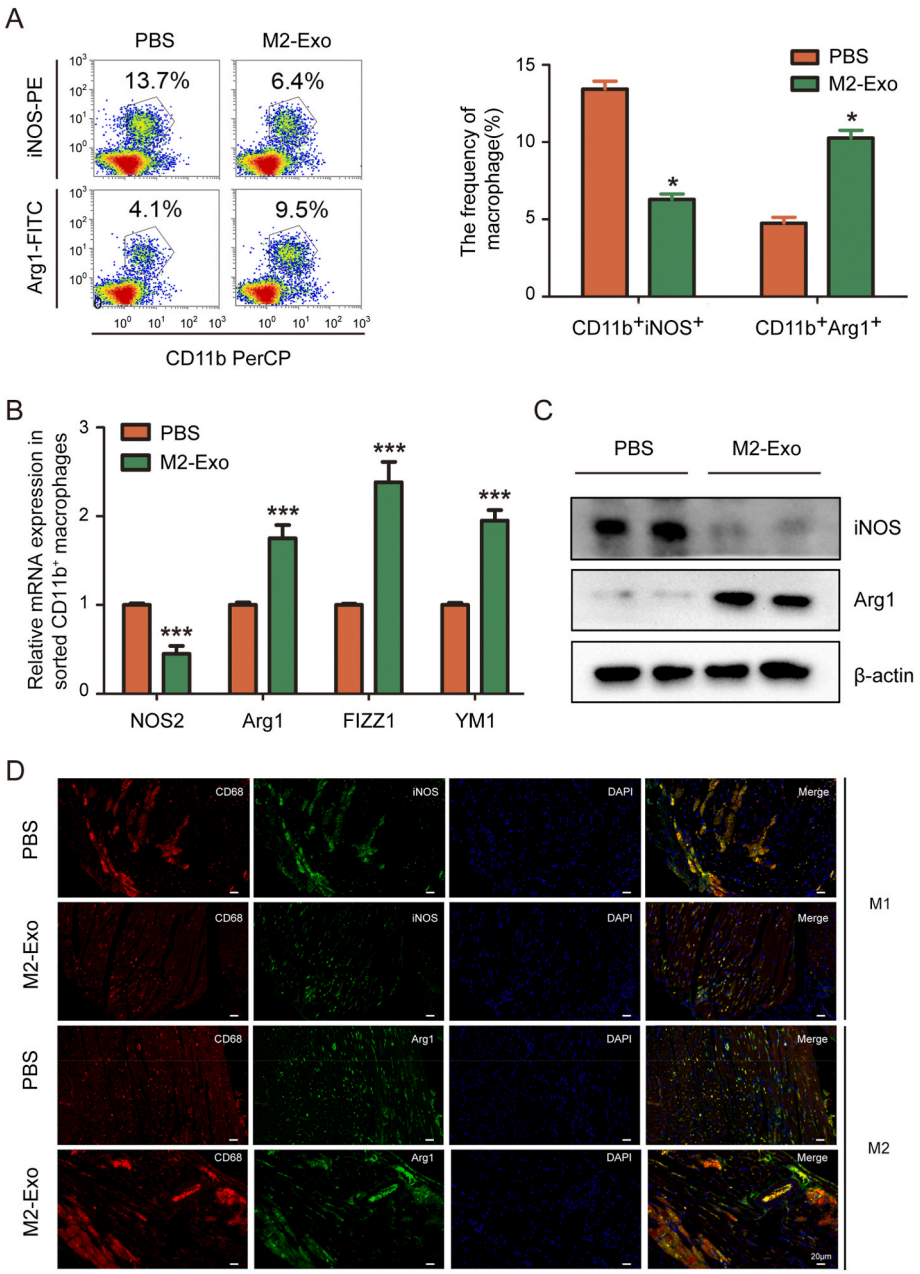

Fig. 2. Effects of M2-Exo on macrophage infiltration and polarization following VM. Mice were intramyocardially injected with PBS or M2-Exo when the VM model was constructed. The macrophage phenotypes of the VM models were evaluated. (A) Myocardial infiltrating macrophages were separated from the mice hearts after enzymatic digestion. The percentage of $CD11b^{+}iNOS^{+}$ or $CD11b^{+}Arg1^{+}$ cells was analyzed by flow cytometry. (B) The expression levels of NOS2, Arg1, FIZZ1, and YM1 in sorted $CD11b^{+}$ macrophages were determined by qRT-PCR. (C) The levels of iNOS and Arg1 in the hearts of mice were assessed by Western blot. (D) On day 7 of the VM models, the mice hearts were made into paraffin slices. Then CD68 (red, macrophage marker), iNOS (green, M1 marker), and Arg1 (green, M2 marker) were detected by immunofluorescence. DAPI was used as the nuclear stain (blue). Scale bar = 100 μm. The experiment was repeated three times with 10–15 mice in each group. Data are presented as the mean ± SD; *P < 0.05, ***P < 0.001.

3.8. AK083884 physically binds with PKM2 and is pivotal to glycolysis metabolic reprogramming

Nuclear-localized lncRNAs always perform their biological functions by acting as molecular scaffolds bridging interactions with proteins. RNA is selectively transferred into the exosomes through RBPs (RNA-binding proteins) [41]. As shown in Fig. 3E, AK083884 was mainly in the nucleus. Therefore, we used RNA pull-down and mass spectrometry (MS) assays to detect AK083884-interacting proteins (Fig. 6A). After intersecting the differentially expressed genes (DEGs) in M2 macrophages and proteins in MS analysis, we focused on an RNA-binding candidate, pyruvate kinase isoform M2 (PKM2) (Fig. 6B). Next, we confirmed the interaction of AK083884 and PKM2 in vivo. PKM2 RNA-binding protein immunoprecipitation (RIP) in noncrosslinked BMDMs, followed by RT-qPCR analysis of copurified RNAs. The results showed that compared to IgG control, AK083884 was specifically enriched in PKM2 antibody immunoprecipitation products (Fig. 6C).

It has been reported that PKM2 is an important determinant of macrophages glycolysis reprogramming. Metabolic reprogramming also participates in regulating macrophage activation and plasticity [42]. Therefore, we further explored whether AK083884 affects the glycolytic function of macrophages by interacting with PKM2. Seahorse XF24 Cell Mito Stress and Glycolysis Stress Test was used to measure the glucose metabolism. As shown in Fig. 6D and E, the glycolytic ability and

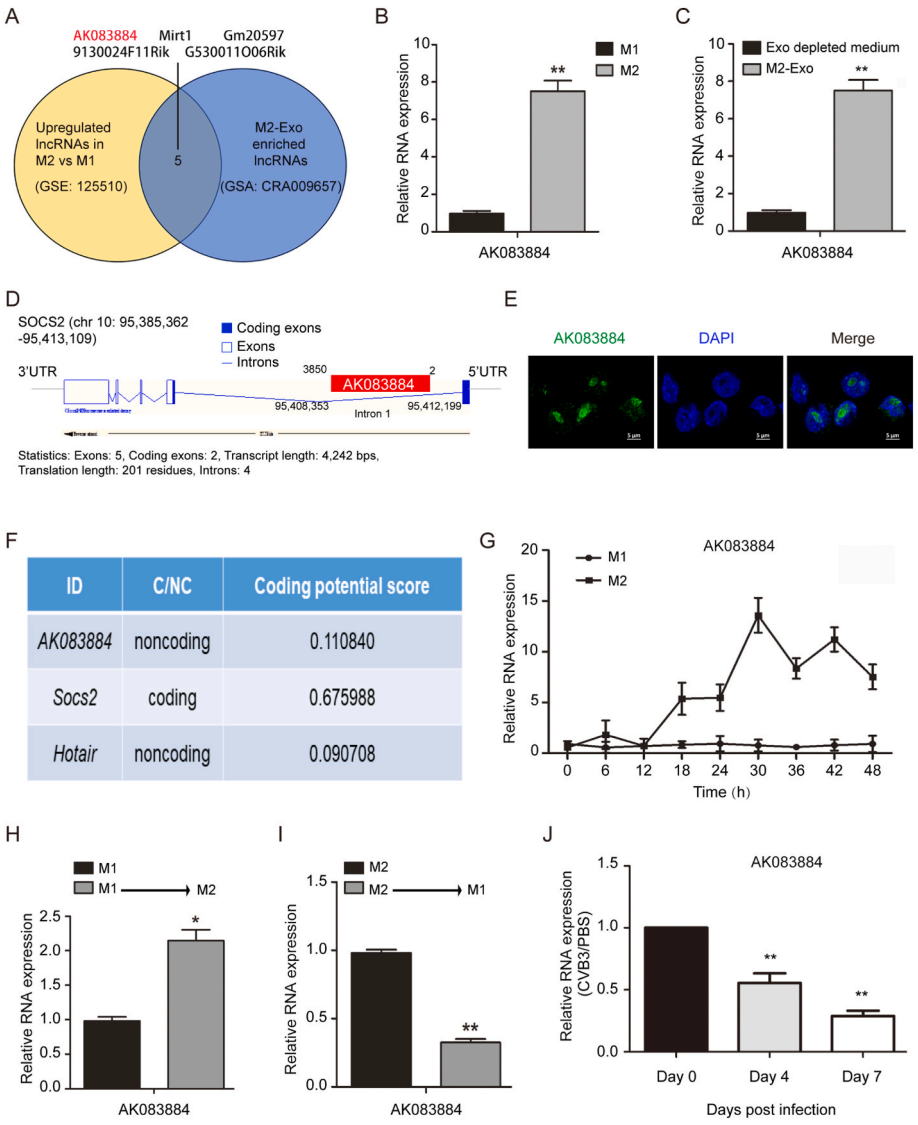

Fig. 3. Characterization of lncRNA AK083884. (A) After identifying the intersection of upregulated lncRNAs in M2 macrophage polarization and enriched lncRNAs in M2-Exo by lncRNA-sequencing analysis, lncRNA AK083884 was selected for further analysis. (B) Expression levels of AK083884 in M1 and M2 macrophages were determined by qRT-PCR. GAPDH was used as an internal control. (C) qRT-PCR analysis of AK083884 level in M2-Exo. (D) AK0883884 was located at the second intron of the SOCS2 gene on mouse chromosome 10. (E) RNA FISH was used to detect endogenous AK083884 (green) in BMDMs. The DNA (blue) was stained with DAPI. Scale bar = 5 μm. (F) The coding potential of AK083884, SOCS2, and HOTAIR was predicted by the CPC program. Both AK083884 and HOTAIR were predicted to be non-coding RNAs, while SOCS2 RNA was predicted to be a coding gene. (G) The time-course expression analysis of AK083884 during M1 or M2 macrophage polarization. (H) Expression levels of AK083884 were determined by qRT-PCR in macrophages following M1-to-M2 re-polarization by IL-4 for 24 h. (I) Expression levels of AK083884 were determined by qRT-PCR in macrophages following M2-to-M1 repolarization by LPS plus IFN-γ for 24 h. (J) The expression of AK083884 in mice heart tissues during VM (n = 3/group). The experiment was repeated three times. Data are presented as the mean ± SD. *P < 0.05, **P < 0.01.

oxidative phosphorylation (OXPHOS) of M2 macrophages were significantly reduced with PKM2 silencing. ECAR assay indicated that AK083884 knockdown significantly promoted non-glycolytic acidification, glycolysis, and glycolytic ability in M2 macrophages, while AK083884 knockdown inhibited the maximal respiration in the OCR assay. Moreover, PKM2 silencing in M2 macrophages significantly reversed the promotional effect of si-AK083884 on glycolysis. In addition, decreased maximal respiration in the si-AK083884 group was enhanced by PKM2 downregulation. Furthermore, we found that PKM2 knockdown inhibited lactate production, while AK083884 knockdown increased lactate production in M2 macrophages. Increased levels of lactate in the si-AK083884 group were reversed by PKM2 knockdown in M2 macrophages (Fig. 6F). In addition, the mRNA levels of M1 marker genes (IL-12, NOS2, and TNF-α) were decreased, whereas the mRNA levels of M2 marker genes (Arg1, FIZZ1, and YM1) were increased when PKM2 was silenced (Fig. 6G and H). These collected data demonstrated that AK083884 may participate in the metabolic reprogramming of M2 macrophages by physically binds with PKM2.

3.9. AK083884 targets PKM2 and regulates PKM2-HIF-1α interaction

To further confirm PKM2 is a target of AK083884 in macrophages, the PKM2 expression in macrophages transfected with AK083884 smart silencer was measured by qRT-PCR and Western blot. The protein level of PKM2 was significantly increased, but there was no significant difference in the transcription level of PKM2 in the M2 macrophages with AK083884 knockdown (Fig. 7A and B).

Previous studies have indicated that PKM2 interacts with HIF-1α and acts as a co-activator of HIF-1α to promote the expression of genes involved in glycolytic metabolism [43]. In our research, PKM2 was

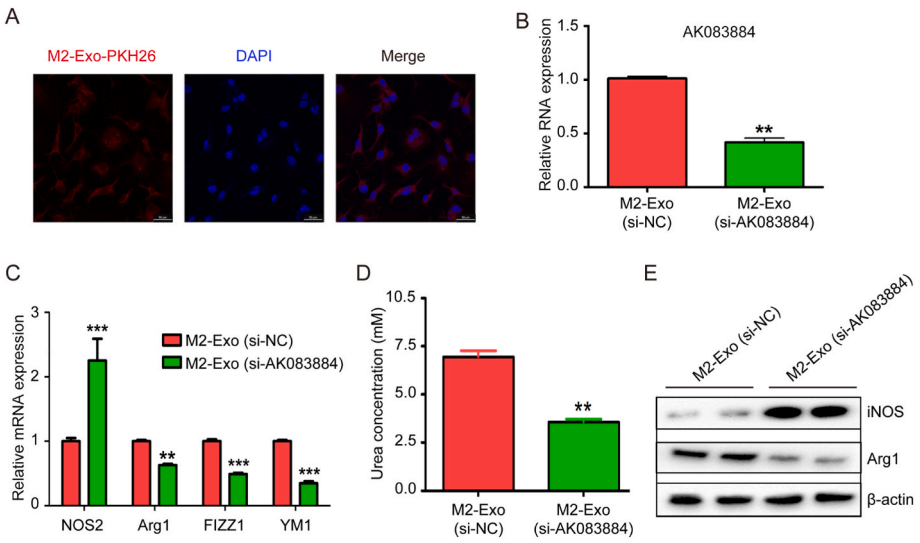

Fig. 4. AK083884 is involved in M2-Exo mediated macrophage polarization *in vitro*. (A) Detection of PKH26 (red)-labeled M2-Exo in BMDMs by immunofluorescence. Scale bar = 50 μm. (B) Knockdown of AK083884 in M2-Exo. We first transfected BMDMs with NC or AK083884 smart silencer for 48h, then polarized with IL-4 toward M2 macrophages for additional 48h, and subsequently purified the exosomes from the culture supernatants of M2 macrophages to acquire M2-Exo (si-NC) and M2-Exo (si-AK083884). AK083884 expression in M2-Exo (si-NC) or M2-Exo (si-AK083884) was assessed by qRT-PCR. (C) Co-culture of BMDMs with M2-Exo (si-NC) or M2-Exo (si-AK083884) for 48 h. Effect of AK083884 knockdown on the expression of M1 marker (NOS2) and M2 markers (Arg1, FIZZ1, and YM1) was detected by qRT-PCR. (D) The arginase activity of M2 markers was assessed by urea production in BMDMs treated with M2-Exo (si-NC) or M2-Exo (si-AK083884). (E) Western blot was used to assess levels of M1 marker iNOSand M2 marker Arg1 in the BMDMs after culturing with M2-Exo (si-NC) or M2-Exo (si-AK083884). The experiment was repeated three times. Data are presented as the mean ± SD. **P < 0.01, ***P < 0.001.

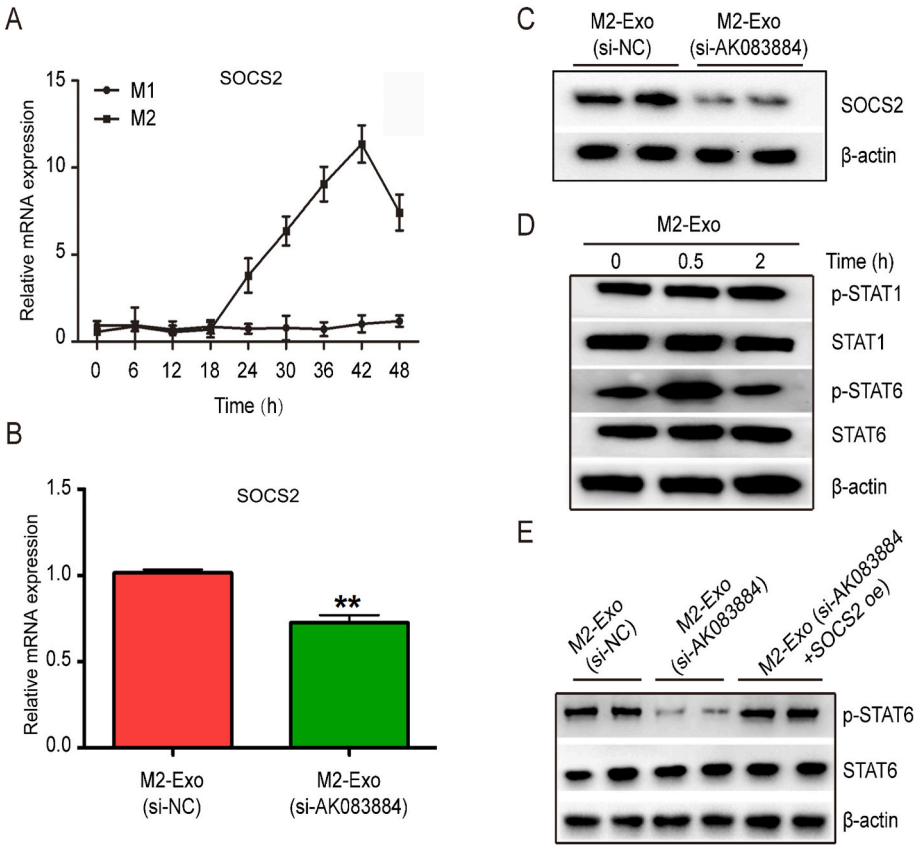

Fig. 5. AK083884 in M2-Exo mediates STAT signaling through targeting SOCS2. (A) Time course of SOCS2 expression in M1 or M2 macrophages. (B) qRT-PCR and (C) Western blot were used to determine the expression of SOCS2 in BMDMs with M2-Exo (si-NC) or M2-Exo (si-AK083884) treatment. (D) BMDMs were treated with M2-Exo for 0, 0.5, and 2 h, and phospho-STAT1 and phospho-STAT6 were detected. (E) Effects of SOCS2 overexpression on phospho-STAT6 expression level in BMDMs with different group M2-Exo treatment. The experiment was repeated three times. Data are presented as the mean ± SD. **P < 0.01.

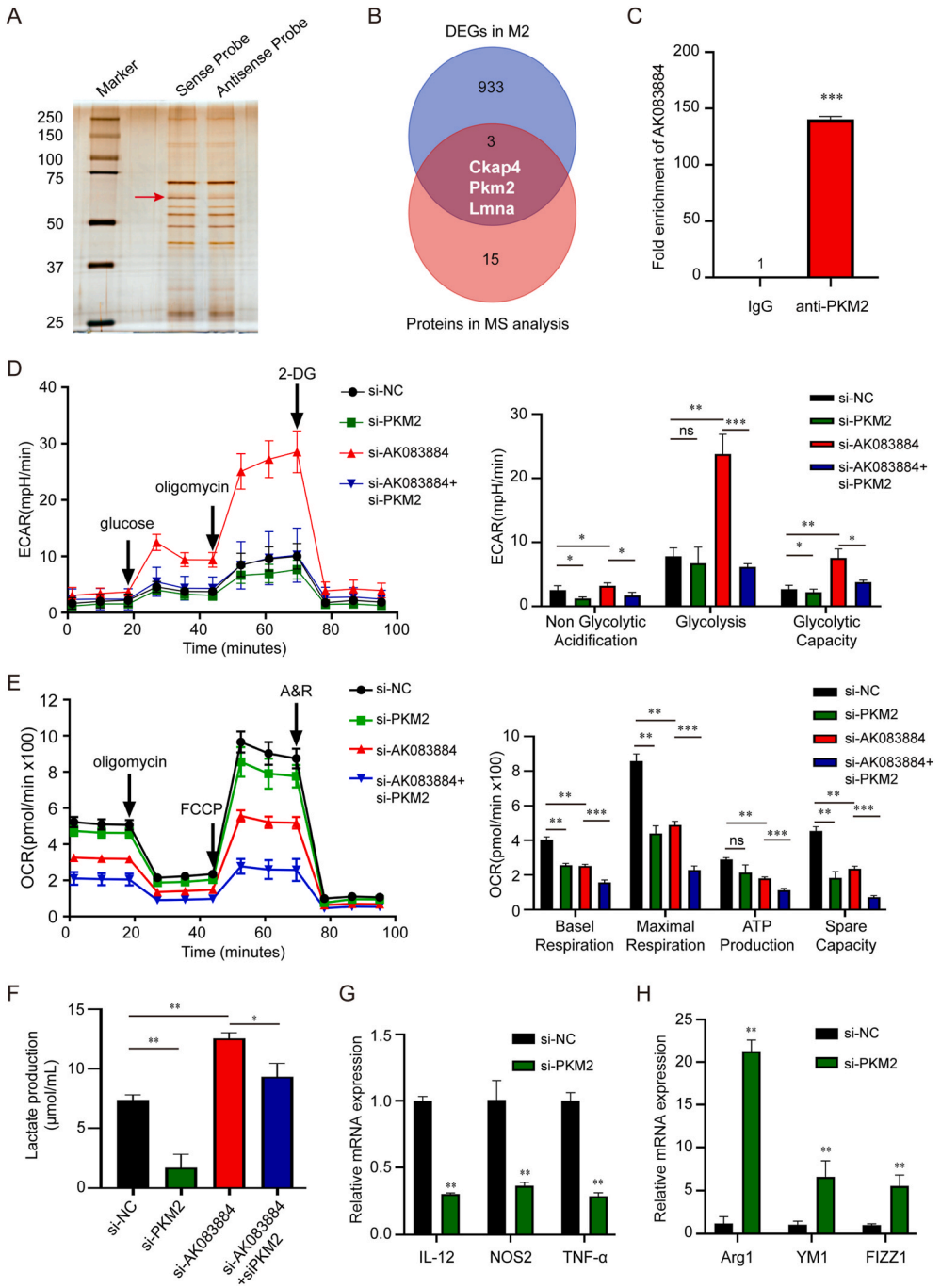

Fig. 6. AK083884 physically binds with PKM2 and is pivotal to glycolysis metabolic reprogramming. (A) Pull-down assay was used to detect the proteins binding with AK083884. Mass spectrometry analysis of proteins with differences in silver staining of SDS-PAGE. (B) After taking the intersection of DEGs in M2 macrophages and proteins in mass spectrometry analysis, PKM2 was selected for further analysis. (C) RIP assay using an anti-PKM2 antibody showed that PKM2 interacted with AK083884 in M2 macrophages. (D) Effects of AK083884 and PKM2 knockdown on the extracellular acidification rate (ECAR) in M2 macrophages. Left panels: ECAR traces were obtained using a Seahorse XF24 Analyzer. Right panels: Statistical analysis of non-glycolytic acidification, glycolysis, and glycolytic ability of the ECAR. 2-DG, 2-deoxy-d-glucose. (E) Effects of AK083884 and PKM2 knockdown on the oxygen consumption rate (OCR) in M2 macrophages. Left panels: OCR traces were detected using a Seahorse XF24 Analyzer. Right panels: Statistical analysis of baseline respiratory capacity, maximum respiratory capacity, ATP-coupled respiratory capacity, and spare reserve respiratory capacity of the OCR. FCCP, carbonyl cyanide-4 (trifluoromethoxy) phenylhydrazone. A & R, antimycin plus rotenone. (F) Effects of AK083884 and/or PKM2 knockdown on lactate production in M2 macrophages. (G, H) BMDMs were transfected with NC or PKM2 siRNAs for 48h, then polarized with LPS + IFN-γ toward M1 macrophages for additional 24h or IL-4 toward M2 macrophages for additional 48h. qRT-PCR was used to detect the expression levels of M1 markers (IL-12, NOS2, TNF-α) in M1 macrophages and M2 markers (Arg1, YM1, and FIZZ1). The experiment was repeated three times. Data are presented as the mean ± SD. ns: no statistical significance, *P < 0.05, **P < 0.01, ***P < 0.001.

downstream of AK083884 and contributed to macrophage polarization. Thus, we further examined whether AK083884 regulated the PKM2/HIF-1α pathway. First, we performed a co-IP to confirm that PKM2 interacts with HIF-1α in BMDMs (Fig. 7C). Then we explored whether AK083884 could affect the interaction between PKM2 and HIF-1α. AK083884 knockdown remarkably enhanced the interaction between PKM2 and HIF-1α (Fig. 7D). In addition, the expression of HIF-1α-targeted genes involved in glycolysis, including glucose

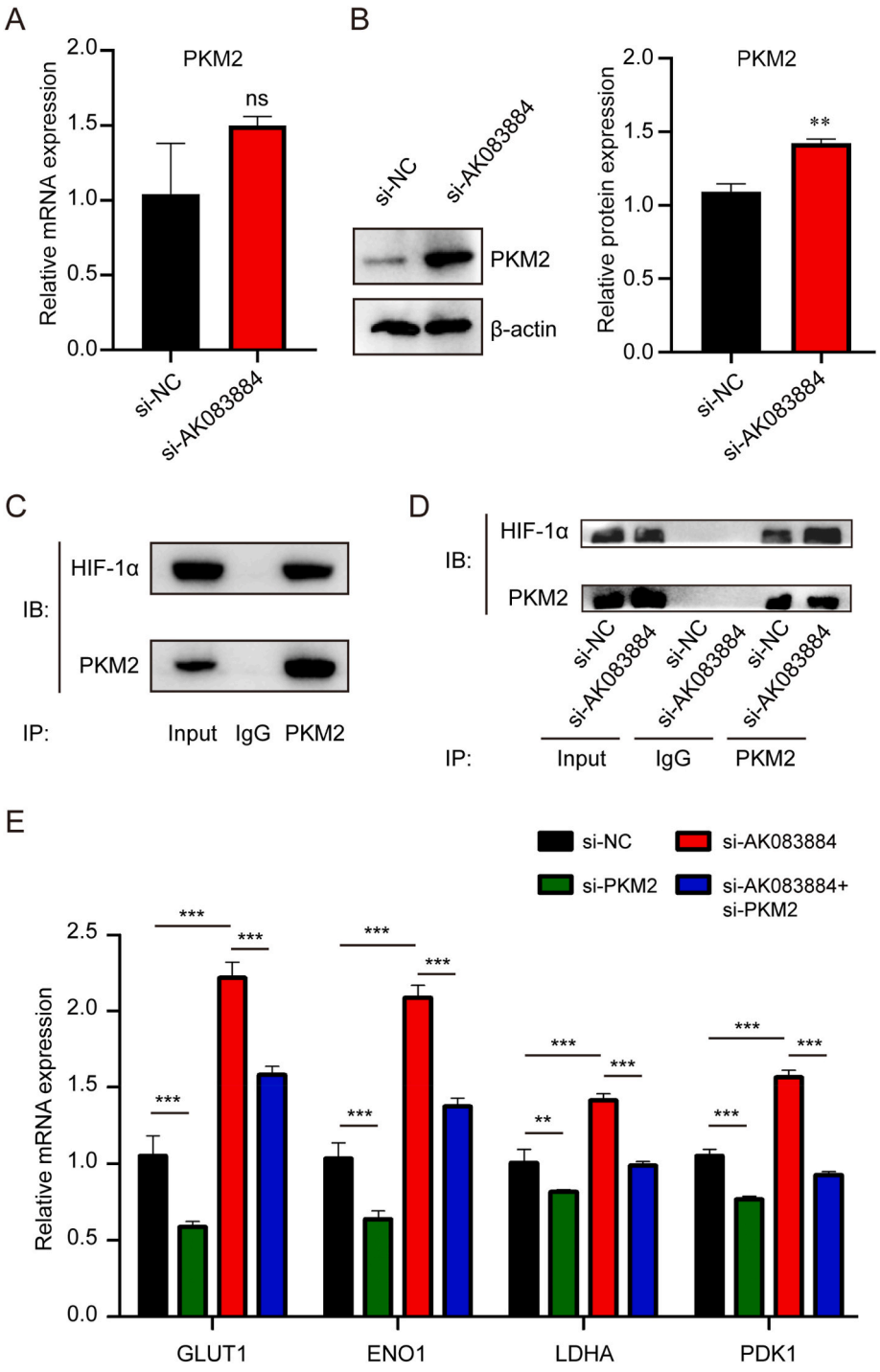

Fig. 7. AK083884 interacts with PKM2 and regulates PKM2-HIF-1α interaction. Effects of AK083884 knockdown on PKM2 expression in M2 macrophages. (A) PKM2 expression was assessed by qRT-PCR. (B) PKM2 expression was assessed by Western blot. (C) Co-IP assay was performed to examine the interaction of HIF-1α and PKM2 in M2 macrophages. (D) Co-IP assay was performed to examine the effects of AK083884 knockdown on PKM2-HIF-1α interaction in M2 macrophages. (E) The expression levels of GLUT1, ENO1, LDHA, and PDK1 in M2 macrophages were measured following knockdown of AK083884 and/or PKM2 by qRT-PCR. The experiment was repeated three times. Data are presented as the mean ± SD. ns: no statistical significance, $^{**}P < 0.01$, $^{***}P < 0.001$.

transporter-1 (GLUT1), enolase 1 (ENO1), lactate dehydrogenase A (LDHA) and pyruvate dehydrogenase kinase 1 (PDK1), was detected. We found that the expression of these genes in M2 macrophages was decreased in response to the inhibition of PKM2, while it was significantly increased with AK083884 knockdown. Moreover, induction of these genes in the si-AK083884 group was counteracted by PKM2 downregulation (Fig. 7E). Taken together, these data indicated that AK083884 may be involved in glycolysis metabolic reprogramming by regulating PKM2-HIF-1α interaction.

3.10. AK083884 is required for myocardial protection exerted by M2-Exo

To explore the role of AK083884 in the myocardial protection exerted by M2-Exo in vivo, we constructed the VM model in BALB/c mice and detected the populations of M1 and M2 phenotypes after M2-

Exo (si-NC) or M2-Exo (si-AK083884) treatment (Fig. 8A). The M1 macrophages ($CD11b^+iNOS^+$) were remarkably increased in mice of the M2-Exo (si-AK083884) group as compared with the M2-Exo (si-NC) group. The M2 macrophages ($CD11b^+CD206^+$) were reduced by AK083884 knockdown. Our results suggested that AK083884 was responsible for the M2-Exo-mediated macrophage polarization in VM.

In addition, we investigated whether inhibition of AK083884 affects inflammation of myocarditis and myocardial function of VM mice with M2-Exo treatment. Compared with the M2-Exo (si-NC) group, H&E staining showed that the area of focal inflammatory cell infiltration among cardiomyocytes was significantly increased in the M2-Exo (si-AK083884) group of mice (Fig. 8B). On week 5, we performed ultrasonic cardiography (UCG) examinations on VM mice. Following AK083884 silencing, the left ventricular ejection fraction and fractional shortening were significantly reduced (Fig. 8C and D). Altogether, our results suggested that AK083884 might be the critical regulatory cargo in M2-Exo responsible for the regulation of macrophage polarization and cardioprotective effects.

4. Discussion

In this study, we first confirmed the curative effects of M2-Exo in CVB3-induced VM. Then we conducted the macrophage depletion model to show that macrophages were the main downstream target of M2-Exo. Our study further demonstrated that M2-Exo effectively promoted polarization of macrophages favorable to M2 rather than M1 phenotype, which might attenuate inflammation, thereby reducing mortality and cardiac dysfunction. Furthermore, we revealed that the lncRNA AK083884 was abundant in M2-Exo and regulated macrophage phenotypes and the SOCS2/STAT signaling pathway. Mechanistic investigations identified that AK083884 directly interacted with PKM2 and regulated PKM2-HIF-1α interaction.

VM is an inflammatory disease characterized by inflammatory infiltration, myocyte degeneration, and necrosis of non-ischemic origin, causing cardiac dysfunction. After CVB3 infection, infiltration of innate (NK cells, macrophages, neutrophils) and adaptive (T cells and B cells) immune cells causes tissue damage by releasing inflammatory cytokines. Among them, macrophages have high plasticity and heterogeneity in the regulation of inflammation. Th2 cytokines can contribute to cardiac remodeling and alleviate myocardial inflammation by promoting M2 macrophages [2]. However, the precise mechanism between M2 macrophages and VM has not been fully clarified. Thereby, whether M2 macrophages or its production play an immunomodulatory role in the inflammation of VM needs to be determined directly.

Previous studies have shown that exosomes can significantly affect anti-inflammatory responses. Mesenchymal stem cell (MSC)-derived exosomes have been shown to exert an anti-inflammatory role on T and B lymphocytes in inflammatory arthritis [44]. Exosomes from adipose-derived stem cells (ADSCs) transferred into macrophages polarize macrophages to an anti-inflammatory M2 phenotype and attenuate adipose inflammation [45]. miR-181c in human umbilical cord MSC (hUCMSC) exosomes has been demonstrated to play a pivotal role in burn-induced inflammation [46]. Moreover, recent studies have indicated that stem cell-derived exosomes can improve global heart

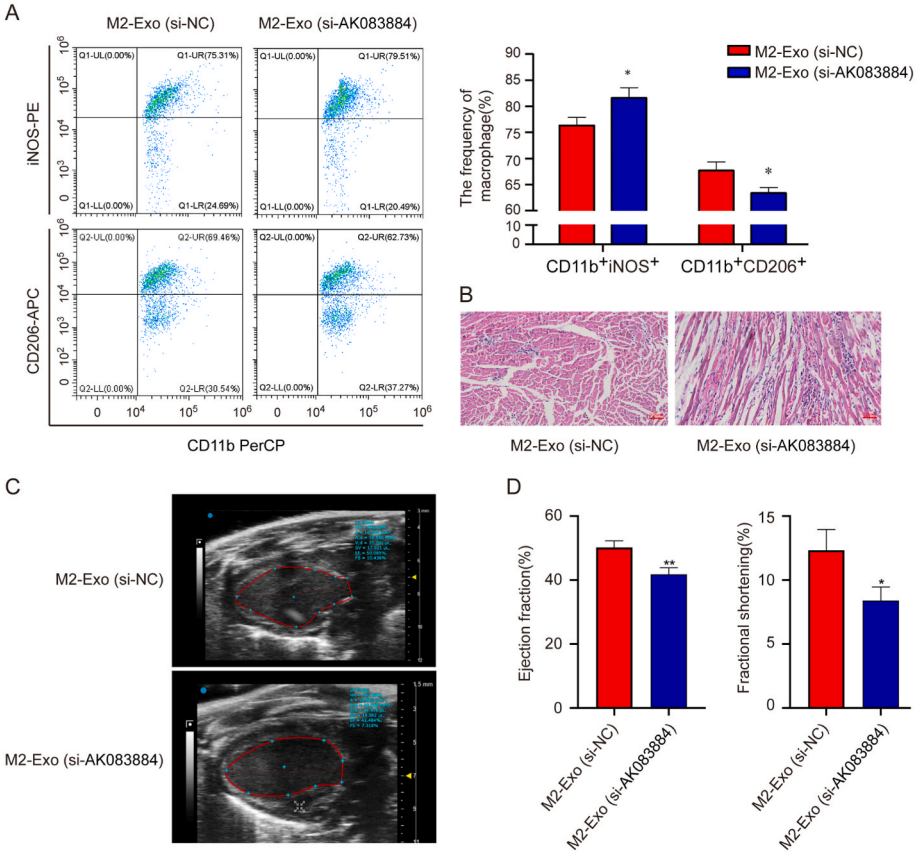

Fig. 8. Knockdown of AK083884 in M2-Exo reduced the efficacy of M2-Exo therapy *in vivo*. Mice were intramyocardially injected with M2-Exo (si-NC) or M2-Exo (si-AK083884) when the VM model was constructed. The phenotypes of the VM models were evaluated. (A) Myocardial infiltrating macrophages were separated from the mice hearts after enzymatic digestion. The percentage of $CD11b^+iNOS^+$ or $CD11b^+CD206^+$ cells was analyzed by flow cytometry. (B) H&E staining of hearts from mice sacrificed on day 7 of VM model. Scale bar = 0.05 mm. (C, D) Cardiac function was measured on left ventricular long axis B-mode images. Echocardiographic analysis of ejection fraction and fractional shortening of mice from each group. The experiment was repeated three times. Data are presented as the mean ± SD. ns, no statistical significance, *P < 0.05, **P < 0.01.

function and alleviate ventricular remodeling by repressing stress-induced apoptosis, diminishing oxidative stress, and activating angiogenesis [47]. However, the function of M2-Exo on VM inflammation has been rarely examined. In our study, M2-Exo treatment not only decreased the inflammatory infiltration and the levels of inflammatory cytokines (IFN-γ, IL-4, and IL-13) but also improved the cardiac function in VM mice.

Accumulating evidence has confirmed that macrophage polarization plays a critical role in CVB3-induced VM. In our work, we conducted a macrophage depletion model and identified that the function of M2-Exo largely depends on their interactions with macrophages. Our previous studies have emphasized that M1 macrophages exacerbate myocarditis, whereas M2 macrophages attenuate myocardial inflammation [16,17]. Furthermore, our study demonstrated that M2-Exo effectively promote the polarization phenotype of macrophage from M1 toward M2 in VM mice. Therefore, the protective effect of M2-Exo in the VM model may be related to its modulation of macrophages.

Exosomes govern intercellular communication by transporting bioactive cargoes (proteins, RNA, lipids, and metabolites) from donor cells to recipient cells in physiological and pathological conditions [23,24]. The functions of exosomal components (proteins and ncRNAs) on macrophage polarization and immune response have been reported. Recently, Ren et al. found that Schwann cell-derived exosomal MFG-E8 modified macrophage/microglial M2 polarization for attenuating inflammation in spinal cord injury [48]. Lu et al. found that a novel tRNA-derived fragment tRF-3022b modulates M2 macrophage polarization contribute to colorectal cancer progression [49]. Liu et al. found that hepatocyte-derived exosomal miR-192–5p plays a critical role in the activation of M1 macrophages polarization and disease progression of nonalcoholic fatty liver disease (NAFLD) [50]. Fan et al. found that exosome encapsulated with mitochondrial circRNA mSCAR promoting M2 macrophage polarization and thus attenuating sepsis [51]. lncRNAs have been confirmed as critical components of exosomes and largely determine the function of exosomes in recipient cells. Previous studies have found that lncRNAs in exosomes derived from macrophages, such as lncRNA AGAP2-AS1 and lncRNA MSTRG.91634.7, have important immunomodulatory properties [52,53]. Probing our lncRNA sequencing of M2-Exo against the upregulation of lncRNA in M2 macrophages, we identified lncRNA AK083884 as our best candidate. Research on the relationship between AK083884 and VM is still limited. The effects of AK083884 on the immunomodulatory function of M2-Exo remain unknown. Our results first indicated that AK083884 inhibition in M2-Exo altered the immunomodulatory effects of M2-Exo on macrophages.

According to the genomic location of lncRNAs relative to adjacent protein-coding genes, lncRNAs can be divided into antisense, intron, intergenic, divergent, and enhancer lncRNA [54]. AK083884 was defined as an intron lncRNA located in the intron 1 region of the SOCS2 on chromosome 10. lncRNAs mainly interact with mRNAs, proteins, and miRNAs to regulate gene expression at multiple levels, such as epigenetics, transcription, post-transcriptional, translation, and post-translational [54]. Studies have shown that SOCS2 affects macrophages during nonalcoholic steatohepatitis or traumatic brain injury. IL-4 induces SOCS2 protein expression in a STAT6-dependent manner [39,55,56]. In our study, we found that the expression of SOCS2 was increased in M2 macrophages. Our data further confirmed that SOCS2 and its downstream STAT6 signaling in macrophages with M2-Exo treatment were negatively regulated by AK083884 knockdown. These data indicated that AK083884 may be involved in the M2-Exo-mediated macrophage polarization by targeting the SOCS2/STAT6 signaling cascades.

The phenotype and functional changes in macrophages are accompanied by dynamic changes in cell metabolism. M1 macrophages are defined by enhanced aerobic glycolysis and reduced OXPHOS, while increased OXPHOS and fatty acid oxidation are the major metabolic features of M2 macrophages [57]. Our study confirms that AK083884 was highly expressed in M2 macrophages, and AK083884 knockdown promoted metabolic reprogramming. By screening and validation, PKM2, a key glycolytic enzyme, was determined as an interaction protein of AK083884. Research has shown that the expression levels of PKM2 were induced in BMDMs with LPS stimulation for 48 h. Knockdown of PKM2 was associated with a decrease in LPS-induced glycolysis [58]. Our research showed that inhibition of PKM2 reduced the glycolytic capacity of M2 macrophages and confirmed that inhibition of PKM2 alleviated pro-inflammatory M1 macrophage phenotype and promoted anti-inflammatory M2 macrophage phenotype. AK083884 may regulate macrophage polarization through metabolic reprogramming. Furthermore, we found that knockdown the expression of SOCS2 did not affect both mRNA and protein expression of PKM2 (data not shown). We speculate that AK083884 may not affect PKM2 signaling pathway through SOCS2. Therefore, we think that AK083884 may function on macrophage polarization through these two signaling pathways, respectively.

The underlying mechanisms of AK083884 function in macrophage metabolic reprogramming have not been elucidated. Thus, we investigated the relationship between the expression of PKM2 and AK083884. We observed that AK083884 could negatively regulate the protein levels of PKM2. According to previous studies, PKM2 can directly interact with HIF-1α and modulate the HIF-1α-dependent gene transcription of enzymes essential for aerobic glycolysis in macrophages. PKM2/HIF-1α plays a pivotal role in the process of M1/M2 polarization. The interaction between PKM2 and HIF-1α in macrophages has been confirmed [42,43]. AK083884 knockdown enhanced the PKM2/HIF-1α interaction, consequently regulating gene transcription in the HIF-1α system. AK083884 might function as a molecular chaperone for PKM2 to interact with HIF-1α.

5. Conclusions

In summary, our study demonstrates that M2-Exo attenuated VM via polarizing M1 macrophages toward M2 macrophages within the heart. AK083884 contained in M2-Exo is involved in the regulation of macrophage polarization by targeting the SOCS2/STAT6 signaling pathway. In this study, we identified that AK083884 directly binds with PKM2 and functions on glycolysis metabolic reprogramming. Furthermore, AK083884 could regulate the interaction of PKM2 with HIF-1α and further modulate the target genes of HIF-1α.

CRediT authorship contribution statement

Yingying Zhang: Investigation. **Liangyu Zhu:** Investigation. **Xueqin Li:** Investigation. **Chang Ge:** Investigation. **Weiya Pei:** Investigation. **Mengying Zhang:** Investigation. **Min Zhong:** Investigation. **Xiaolong Zhu:** Writing – original draft. **Kun Lv:** Writing – review & editing.

Declaration of competing interest

The authors declare that they have no conflicts of interest concerning this article.

Data availability

Data will be made available on request.

Acknowledgments

This work was supported by the National Natural Science Foundation of China (82170368, 82072370 and 82100019), Innovation fund for Industry-University-Research of Chinese universities (2023HT008), Natural Science Foundation of Anhui Province (2108085J44, 2308085MH261, 2108085QH307), Program for Excellent Sci-tech Innovation Teams of Universities in Anhui Province (2022AH010074),

Major Projects of Natural Science Research of Universities in Anhui Province (2022AH040177), Key Projects of Natural Science Research of Universities in Anhui Province (2023AH051769), Science and Technology Project of Wuhu City (2022jc56, 2022jc57 and 2022jc66), Scientific Research Project of Wannan Medical College (RNA202101), Funding of "Peak" Training Program for Scientific Research of Yijishan Hospital, Wannan Medical College (GF2019T01, KPF2019004, GF2019G09 and GF2019G10). We thank LetPub (www.letpub.com) for its linguistic assistance during the preparation of this manuscript.

Appendix A. Supplementary data

Supplementary data to this article can be found online at https://doi.org/10.1016/j.redox.2023.103016.

References

[1] A.M. Feldman, D. McNamara, Myocarditis. N Engl J Med 343 (2000) 1388–1398.
[2] M. Esfandiarei, B.M. McManus, Molecular biology and pathogenesis of viral myocarditis, Annu. Rev. Pathol. 3 (2008) 127–155.
[3] F.S. Garmaroudi, D. Marchant, R. Hendry, H. Luo, D. Yang, X. Ye, J. Shi, B. M. McManus, Coxsackievirus B3 replication and pathogenesis, Future Microbiol. 10 (2015) 629–653.
[4] D. Westermann, K. Savvatis, H.P. Schultheiss, C. Tschope, Immunomodulation and matrix metalloproteinases in viral myocarditis, J. Mol. Cell. Cardiol. 48 (2010) 468–473.
[5] D.J. Marchant, B.M. McManus, Regulating viral myocarditis: allografted regulatory T cells decrease immune infiltration and viral load, Circulation 121 (2010) 2609–2611.
[6] A.P. Papageorgiou, M. Swinnen, D. Vanhoutte, T. VandenDriessche, M. Chuah, D. Lindner, W. Verhesen, B. de Vries, J. D'Hooge, E. Lutgens, D. Westermann, et al., Thrombospondin-2 prevents cardiac injury and dysfunction in viral myocarditis through the activation of regulatory T-cells, Cardiovasc. Res. 94 (2012) 115–124.
[7] A. Valaperti, M. Nishii, Y. Liu, K. Naito, M. Chan, L. Zhang, C. Skurk, H. P. Schultheiss, G.A. Wells, U. Eriksson, P.P. Liu, Innate immune interleukin-1 receptor-associated kinase 4 exacerbates viral myocarditis by reducing CCR5(+) CD11b(+) monocyte migration and impairing interferon production, Circulation 128 (2013) 1542–1554.
[8] D. Fairweather, N.R. Rose, Coxsackievirus-induced myocarditis in mice: a model of autoimmune disease for studying immunotoxicity, Methods 41 (2007) 118–122.
[9] K. Li, W. Xu, Q. Guo, Z. Jiang, P. Wang, Y. Yue, S. Xiong, Differential macrophage polarization in male and female BALB/c mice infected with coxsackievirus B3 defines susceptibility to viral myocarditis, Circ. Res. 105 (2009) 353–364.
[10] L. Liu, Y. Yue, S. Xiong, NK-derived IFN-gamma/IL-4 triggers the sexually disparate polarization of macrophages in CVB3-induced myocarditis, J. Mol. Cell. Cardiol. 76 (2014) 15–25.
[11] X. Hua, G. Hu, Q. Hu, Y. Chang, Y. Hu, L. Gao, X. Chen, P.C. Yang, Y. Zhang, M. Li, J. Song, Single-cell RNA sequencing to dissect the immunological network of autoimmune myocarditis, Circulation 142 (2020) 384–400.
[12] S. Gordon, Alternative activation of macrophages, Nat. Rev. Immunol. 3 (2003) 23–35.
[13] F.O. Martinez, L. Helming, S. Gordon, Alternative activation of macrophages: an immunologic functional perspective, Annu. Rev. Immunol. 27 (2009) 451–483.
[14] D.M. Mosser, J.P. Edwards, Exploring the full spectrum of macrophage activation, Nat. Rev. Immunol. 8 (2008) 958–969.
[15] F.O. Martinez, A. Sica, A. Mantovani, M. Locati, Macrophage activation and polarization, Front. Biosci. 13 (2008) 453–461.
[16] Y. Zhang, X. Li, X. Kong, M. Zhang, D. Wang, Y. Liu, K. Lv, Long non-coding RNA AK085865 ablation confers susceptibility to viral myocarditis by regulating macrophage polarization, J. Cell Mol. Med. 24 (2020) 5542–5554.
[17] Y. Zhang, M. Zhang, X. Li, Z. Tang, X. Wang, M. Zhong, Q. Suo, Y. Zhang, K. Lv, Silencing MicroRNA-155 attenuates cardiac injury and dysfunction in viral myocarditis via promotion of M2 phenotype polarization of macrophages, Sci. Rep. 6 (2016), 22613.
[18] X. Yang, Y. Yue, S. Xiong, Dpep2 emerging as a modulator of macrophage inflammation confers protection against CVB3-induced viral myocarditis, Front. Cell. Infect. Microbiol. 9 (2019) 57.
[19] C. Wang, C. Dong, S. Xiong, IL-33 enhances macrophage M2 polarization and protects mice from CVB3-induced viral myocarditis, J. Mol. Cell. Cardiol. 103 (2017) 22–30.
[20] W. Gou, Z. Zhang, C. Yang, Y. Li, MiR-223/Pknox1 axis protects mice from CVB3-induced viral myocarditis by modulating macrophage polarization, Exp. Cell Res. 366 (2018) 41–48.
[21] Y. Li, Y. Huang, W. Wu, B. Wei, L.B. Qin, Cells increase myocardial inflammation by suppressing M2 macrophage polarization in coxsackie virus B3-induced acute myocarditis, Inflammation 42 (2019) 953–960.
[22] R. Gallet, J. Dawkins, J. Valle, E. Simsolo, G. de Couto, R. Middleton, E. Tseliou, D. Luthringer, M. Kreke, R.R. Smith, L. Marban, et al., Exosomes secreted by cardiosphere-derived cells reduce scarring, attenuate adverse remodelling, and improve function in acute and chronic porcine myocardial infarction, Eur. Heart J. 38 (2017) 201–211.
[23] P. Mathiyalagan, Y. Liang, D. Kim, S. Misener, T. Thorne, C.E. Kamide, E. Klyachko, D.W. Losordo, R.J. Hajjar, S. Sahoo, Angiogenic mechanisms of human CD34(+) stem cell exosomes in the repair of ischemic hindlimb, Circ. Res. 120 (2017) 1466–1476.
[24] R.C. Lai, T.S. Chen, S.K. Lim, Mesenchymal stem cell exosome: a novel stem cell-based therapy for cardiovascular disease, Regen. Med. 6 (2011) 481–492.
[25] S. Sahoo, D.W. Losordo, Exosomes and cardiac repair after myocardial infarction, Circ. Res. 114 (2014) 333–344.
[26] J.P. Sluijter, E. van Rooij, Exosomal microRNA clusters are important for the therapeutic effect of cardiac progenitor cells, Circ. Res. 116 (2015) 219–221.
[27] Y. Wang, L. Zhang, Y. Li, L. Chen, X. Wang, W. Guo, X. Zhang, G. Qin, S.H. He, A. Zimmerman, Y. Liu, et al., Exosomes/microvesicles from induced pluripotent stem cells deliver cardioprotective miRNAs and prevent cardiomyocyte apoptosis in the ischemic myocardium, Int. J. Cardiol. 192 (2015) 61–69.
[28] Y. Yue, V.N.S. Garikipati, S.K. Verma, D.A. Goukassian, R. Kishore, Interleukin-10 deficiency impairs reparative properties of bone marrow-derived endothelial progenitor cell exosomes, Tissue Eng. 23 (2017) 1241–1250.
[29] B. Liu, B.W. Lee, K. Nakanishi, A. Villasante, R. Williamson, J. Metz, J. Kim, M. Kanai, L. Bi, K. Brown, G. Di Paolo, et al., Cardiac recovery via extended cell-free delivery of extracellular vesicles secreted by cardiomyocytes derived from induced pluripotent stem cells, Nat. Biomed. Eng. 2 (2018) 293–303.
[30] R. Wu, W. Gao, K. Yao, J. Ge, Roles of exosomes derived from immune cells in cardiovascular diseases, Front. Immunol. 10 (2019) 648.
[31] W. Ying, M. Riopel, G. Bandyopadhyay, Y. Dong, A. Birmingham, J.B. Seo, J. M. Ofrecio, J. Wollam, A. Hernandez-Carretero, W. Fu, P. Li, et al., Adipose tissue macrophage-derived exosomal miRNAs can modulate in vivo and in vitro insulin sensitivity, Cell 171 (2017), 372-384.e312.
[32] Y.W. Choo, M. Kang, H.Y. Kim, J. Han, S. Kang, J.R. Lee, G.J. Jeong, S.P. Kwon, S. Y. Song, S. Go, M. Jung, et al., M1 macrophage-derived nanovesicles potentiate the anticancer efficacy of immune checkpoint inhibitors, ACS Nano 12 (2018) 8977–8993.
[33] L. Cheng, Y. Wang, L. Huang, Exosomes from M1-polarized macrophages potentiate the cancer vaccine by creating a pro-inflammatory microenvironment in the lymph node, Mol. Ther. 25 (2017) 1665–1675.
[34] J. Lan, L. Sun, F. Xu, L. Liu, F. Hu, D. Song, Z. Hou, W. Wu, X. Luo, J. Wang, X. Yuan, et al., M2 macrophage-derived exosomes promote cell migration and invasion in colon cancer, Cancer Res. 79 (2019) 146–158.
[35] S. Liu, J. Chen, J. Shi, W. Zhou, L. Wang, W. Fang, Y. Zhong, X. Chen, Y. Chen, A. Sabri, S. Liu, M1-like macrophage-derived exosomes suppress angiogenesis and exacerbate cardiac dysfunction in a myocardial infarction microenvironment, Basic Res. Cardiol. 115 (2020) 22.
[36] J. Wang, Y. Rong, C. Ji, C. Lv, D. Jiang, X. Ge, F. Gong, P. Tang, W. Cai, W. Liu, J. Fan, MicroRNA-421-3p-abundant small extracellular vesicles derived from M2 bone marrow-derived macrophages attenuate apoptosis and promote motor function recovery via inhibition of mTOR in spinal cord injury, J. Nanobiotechnol. 18 (2020) 72.
[37] L. Bouchareychas, P. Duong, S. Covarrubias, E. Alsop, T.A. Phu, A. Chung, M. Gomes, D. Wong, B. Meechoovet, A. Capili, R. Yamamoto, et al., Macrophage exosomes resolve atherosclerosis by regulating hematopoiesis and inflammation via MicroRNA cargo, Cell Rep. 32 (2020), 107881.
[38] Z. Hu, J. Zhan, G. Pei, R. Zeng, Depletion of macrophages with clodronate liposomes partially attenuates renal fibrosis on AKI-CKD transition, Ren. Fail. 45 (2023), 2149412.
[39] S. Li, S. Han, K. Jin, T. Yu, H. Chen, X. Zhou, Z. Tan, G. Zhang, SOCS2 suppresses inflammation and apoptosis during NASH progression through limiting NF-κB activation in macrophages, Int. J. Biol. Sci. 17 (2021) 4165–4175.
[40] H. Dickensheets, N. Vazquez, F. Sheikh, S. Gingras, P.J. Murray, J.J. Ryan, R. P. Donnelly, Suppressor of cytokine signaling-1 is an IL-4-inducible gene in macrophages and feedback inhibits IL-4 signaling, Gene Immun. 8 (2007) 21–27.
[41] C. Villarroya-Beltri, C. Gutiérrez-Vázquez, F. Sánchez-Cabo, D. Pérez-Hernández, J. Vázquez, N. Martin-Cofreces, D.J. Martinez-Herrera, A. Pascual-Montano, M. Mittelbrunn, F. Sánchez-Madrid, Sumoylated hnRNPA2B1 controls the sorting of miRNAs into exosomes through binding to specific motifs, Nat. Commun. 4 (2013) 2980.
[42] E.M. Palsson-McDermott, A.M. Curtis, G. Goel, M.A. Lauterbach, F.J. Sheedy, L. E. Gleeson, M.W. van den Bosch, S.R. Quinn, R. Domingo-Fernandez, D. G. Johnston, J.K. Jiang, et al., Pyruvate kinase M2 regulates Hif-1α activity and IL-1β induction and is a critical determinant of the warburg effect in LPS-activated macrophages, Cell Metabol. 21 (2015) 65–80.
[43] Q. Hua, B. Mi, F. Xu, J. Wen, L. Zhao, J. Liu, G. Huang, Hypoxia-induced lncRNA-AC020978 promotes proliferation and glycolytic metabolism of non-small cell lung cancer by regulating PKM2/HIF-1alpha axis, Theranostics 10 (2020) 4762–4778.
[44] S. Cosenza, K. Toupet, M. Maumus, P. Luz-Crawford, O. Blanc-Brude, C. Jorgensen, D. Noel, Mesenchymal stem cells-derived exosomes are more immunosuppressive than microparticles in inflammatory arthritis, Theranostics 8 (2018) 1399–1410.
[45] H. Zhao, Q. Shang, Z. Pan, Y. Bai, Z. Li, H. Zhang, Q. Zhang, C. Guo, L. Zhang, Q. Wang, Exosomes from adipose-derived stem cells attenuate adipose inflammation and obesity through polarizing M2 macrophages and beiging in white adipose tissue, Diabetes 67 (2018) 235–247.
[46] X. Li, L. Liu, J. Yang, Y. Yu, J. Chai, L. Wang, L. Ma, H. Yin, Exosome derived from human umbilical cord mesenchymal stem cell mediates MiR-181c attenuating burn-induced excessive inflammation, EBioMedicine 8 (2016) 72–82.
[47] J. Zhao, X. Li, J. Hu, F. Chen, S. Qiao, X. Sun, L. Gao, J. Xie, B. Xu, Mesenchymal stromal cell-derived exosomes attenuate myocardial ischaemia-reperfusion injury through miR-182-regulated macrophage polarization, Cardiovasc. Res. 115 (2019) 1205–1216.

[48] J. Ren, B. Zhu, G. Gu, W. Zhang, J. Li, H. Wang, M. Wang, X. Song, Z. Wei, S. Feng, Schwann cell-derived exosomes containing MFG-E8 modify macrophage/microglial polarization for attenuating inflammation via the SOCS3/STAT3 pathway after spinal cord injury, Cell Death Dis. 14 (2023) 70.
[49] S. Lu, X. Wei, L. Tao, D. Dong, W. Hu, Q. Zhang, Y. Tao, C. Yu, D. Sun, H. Cheng, A novel tRNA-derived fragment tRF-3022b modulates cell apoptosis and M2 macrophage polarization via binding to cytokines in colorectal cancer, J. Hematol. Oncol. 15 (2022) 176.
[50] X.L. Liu, Q. Pan, H.X. Cao, F.Z. Xin, Z.H. Zhao, R.X. Yang, J. Zeng, H. Zhou, J. G. Fan, Lipotoxic hepatocyte-derived exosomal MicroRNA 192-5p activates macrophages through rictor/akt/Forkhead Box transcription factor O1 signaling in nonalcoholic fatty liver disease, Hepatology 72 (2020) 454–469.
[51] L. Fan, L. Yao, Z. Li, Z. Wan, W. Sun, S. Qiu, W. Zhang, D. Xiao, L. Song, G. Yang, Y. Zhang, et al., Exosome-based mitochondrial delivery of circRNA mSCAR alleviates sepsis by orchestrating macrophage activation, Adv. Sci. 10 (2023), e2205692.
[52] F. Zhang, Y. Sang, D. Chen, X. Wu, X. Wang, W. Yang, Y. Chen, M2 macrophage-derived exosomal long non-coding RNA AGAP2-AS1 enhances radiotherapy immunity in lung cancer by reducing microRNA-296 and elevating NOTCH2, Cell Death Dis. 12 (2021) 467.
[53] J. Ban, F. Liu, Q. Zhang, S. Chang, X. Zeng, J. Chen, Macrophage-derived exosomal lncRNA MSTRG.91634.7 inhibits fibroblasts activation by targeting PINK1 in silica-induced lung fibrosis, Toxicol. Lett. 372 (2023) 36–44.
[54] M. Knoll, H.F. Lodish, L. Sun, Long non-coding RNAs as regulators of the endocrine system. Nature reviews, Endocrinology 11 (2015) 151–160.
[55] H.S. Basrai, A.M. Turnley, The suppressor of cytokine signalling 2 (SOCS2), traumatic brain injury and microglial/macrophage regulation, Neural Regen Res 11 (2016) 1405–1406.
[56] U. Sriram, J. Xu, R.W. Chain, L. Varghese, M. Chakhtoura, H.L. Bennett, P. W. Zoltick, S. Gallucci, IL-4 suppresses the responses to TLR7 and TLR9 stimulation and increases the permissiveness to retroviral infection of murine conventional dendritic cells, PLoS One 9 (2014), e87668.
[57] F. Wang, S. Zhang, I. Vuckovic, R. Jeon, A. Lerman, C.D. Folmes, P.P. Dzeja, J. Herrmann, Glycolytic stimulation is not a requirement for M2 macrophage differentiation, Cell Metabol. 28 (2018), 463-475.e464.
[58] L. Yang, M. Xie, M. Yang, Y. Yu, S. Zhu, W. Hou, R. Kang, M.T. Lotze, T.R. Billiar, H. Wang, L. Cao, et al., PKM2 regulates the Warburg effect and promotes HMGB1 release in sepsis, Nat. Commun. 5 (2014) 4436.